

## High-spin states and shell structure of the odd-odd nucleus $^{90}\text{Nb}$

X. Z. Cui,<sup>1,2</sup> L. H. Zhu,<sup>1,\*</sup> X. G. Wu,<sup>1</sup> Z. M. Wang,<sup>1</sup> C. Y. He,<sup>1</sup> Y. Liu,<sup>1,4</sup> G. S. Li,<sup>1</sup> S. X. Wen,<sup>1</sup> Z. L. Zhang,<sup>1,2</sup> R. Meng,<sup>1,2</sup> R. G. Ma,<sup>1</sup> P. Luo,<sup>3</sup> Y. Zheng,<sup>3</sup> M. M. Ndontchueng,<sup>5</sup> J. D. Huo,<sup>2</sup> and C. X. Yang<sup>1,2</sup>

<sup>1</sup>China Institute of Atomic Energy, Beijing 102413, China

<sup>2</sup>College of Physics, Jilin University, Changchun 130021, China

<sup>3</sup>Institute of Modern Physics, Lanzhou 730000, China

<sup>4</sup>The North-East Normal University, Changchun 130024, China

<sup>5</sup>Université de Douala, Faculté de Sciences, B.P. 8580 Cameroun

(Received 3 February 2005; published 31 October 2005)

The high-spin states of the odd-odd nucleus  $^{90}\text{Nb}$  have been investigated with in-beam  $\gamma$ -spectroscopic techniques via the  $^{76}\text{Ge}(^{19}\text{F}, 5n)^{90}\text{Nb}$  reaction at a beam energy of 80 MeV.  $\gamma$ - $\gamma$  coincidences were measured using a  $\gamma$ -ray detector array. Twenty new  $\gamma$  rays have been assigned to  $^{90}\text{Nb}$  and the level scheme has been extended up to an excitation energy of 8.095 MeV at spin  $18\hbar$ . The level structure of  $^{90}\text{Nb}$  at high spin states has been well reproduced using semiempirical shell-model calculations in the model space  $\pi(1p_{1/2}, 0f_{5/2}, 0g_{9/2})\nu(0g_{9/2})$ . The results show that the excitation of protons plays an important role in generating the high-spin states of  $^{90}\text{Nb}$ .

DOI: 10.1103/PhysRevC.72.044322

PACS number(s): 23.20.Lv, 21.60.Cs, 27.60.+j

### I. INTRODUCTION

Angular momentum in nuclei can be constructed in two ways, i.e., intrinsic excitation and collective excitation. The former is dominated by aligned angular momentum of the valence nucleons, whereas the latter is formed by motion of the nucleus as a whole. It is well known that near the proton and/or neutron magic numbers, angular momentum of the nucleus is generated mainly by intrinsic excitations.

A number of studies have revealed that the level structures of nuclei in the  $N \sim 50$ ,  $Z \sim 40$  region can be well described by the shell model [1–10]. For low-lying states, taking  $^{88}\text{Sr}$  as the inert core and the valence nucleons occupying the  $(p_{1/2}, g_{9/2})$  configuration space, the results of shell-model calculations are in good agreement with the observed levels [3,7,10–12]. For the high-spin states, a larger configuration space should be involved and even the excitation of the core has to be taken into account. Therefore, systematic studies of high-spin states in nuclei near the  $N \sim 50$ ,  $Z \sim 40$  region may provide important information on the core excitation mechanism.

The purpose of the present work is to establish the level structure of the odd-odd nucleus  $^{90}\text{Nb}$  at high spin. The low-lying states of  $^{90}\text{Nb}$  had been studied previously [4,6], and the experimental results are consistent with shell-model calculations in which the odd-odd nucleus  $^{90}\text{Nb}$ , with 41 protons and 49 neutrons, has two valence nucleons outside the  $^{88}\text{Sr}$  core, i.e., one proton particle and one neutron hole in  $g_{9/2}$  orbital, respectively. In this article, new experimental results on the high-spin states of  $^{90}\text{Nb}$  are presented and compared to semiempirical shell-model calculations.

### II. EXPERIMENTAL METHODS AND RESULTS

The high-spin states of  $^{90}\text{Nb}$  were populated via the fusion-evaporation reaction  $^{76}\text{Ge}(^{19}\text{F}, 5n)^{90}\text{Nb}$  at a beam energy of 80 MeV. The  $^{19}\text{F}$  beam was delivered by the HI-13 tandem

accelerator of the China Institute of Atomic Energy (CIAE). The target consisted of a 2.2 mg/cm<sup>2</sup> layer of  $^{76}\text{Ge}$  enriched to 96% and evaporated on a 10 mg/cm<sup>2</sup> lead backing. The beam energy was chosen to maximize the yield of  $^{90}\text{Nb}$ , which should be about 28.5% of the total cross section as predicted by the statistical evaporation code CASCADE [13].  $\gamma$ - $\gamma$  coincidence events were collected using a multidetector array consisting of 14 HPGe detectors, each of which was equipped with a BGO Compton suppression shield to enhance the photopeaks relative to the Compton background. In the detector array, four detectors were placed at 90°, five at about 48°, and five at about 132° with respect to the beam direction. Each detector had an energy resolution of about 2 keV for 1332.5-keV  $\gamma$  rays. The relative efficiency of the detector array was calibrated using a  $^{152}\text{Eu}$  standard radioactive source mounted at the target position. A total of  $68 \times 10^6$   $\gamma$ - $\gamma$  coincidence events were collected in the experiment in event-by-event mode. After careful energy calibration and gain matching of each detector, the  $\gamma$ - $\gamma$  coincidence data were sorted offline into conventional  $E_{\gamma_1}$ - $E_{\gamma_2}$  matrices and then analyzed using the RADWARE package [14] based on a Linux-PC system.

#### A. The level scheme of $^{90}\text{Nb}$

$^{90}\text{Nb}$  had previously been studied using  $\alpha$ - and  $^3\text{He}$ -induced reactions [15] and its level scheme was known up to the  $12^-$  state at 2.487 MeV. The 813-keV  $\gamma$  ray, the strongest of  $^{90}\text{Nb}$ , is used as a characteristic  $\gamma$  ray in the  $\gamma$ - $\gamma$  coincidence analysis for the identification of the new  $\gamma$  rays of  $^{90}\text{Nb}$  in present work. The  $\gamma$  rays assigned to  $^{90}\text{Nb}$  from the present experiment are listed in Table I and some typical gated spectra are shown in Fig. 1.

Cascades of  $\gamma$  transitions were determined according to the coincidence relationships and the relative intensities of the  $\gamma$  rays in the gated spectra. The level scheme based on the present experiment is shown in Fig. 2. In addition to the 813-keV  $\gamma$ -ray, 996, 1067, and 607 keV  $\gamma$ -rays reported in Ref. [15] have been also observed, whereas other transitions between low spin states, mostly between  $8^+$  and  $9^+$  states, were

\*Corresponding author: zhulh@iris.ciae.ac.cn

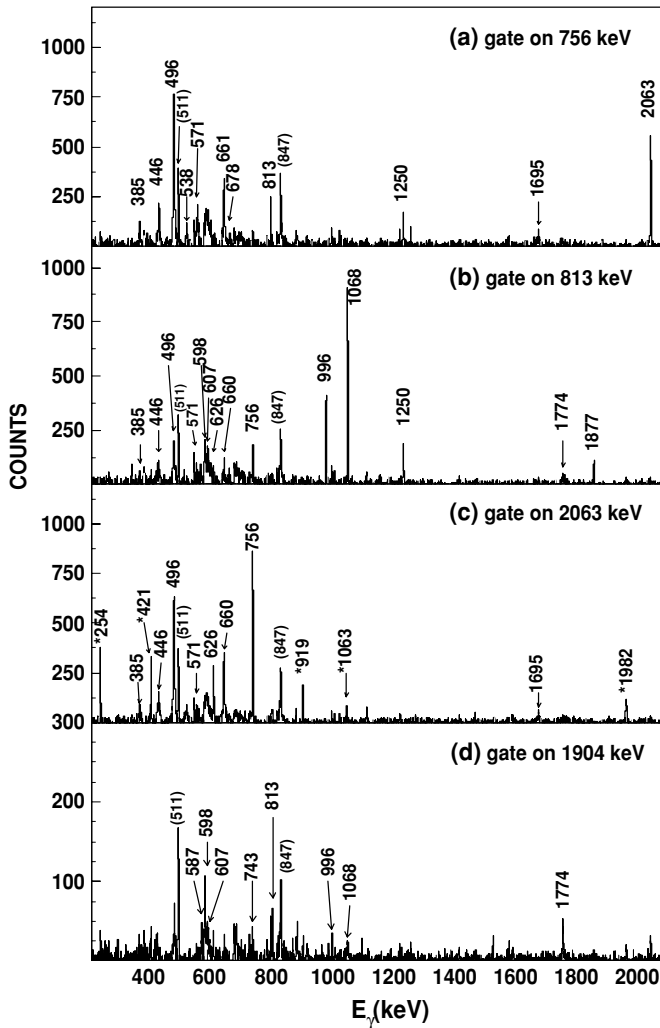


FIG. 1. Prompt  $\gamma$ - $\gamma$  coincidence spectra of  $^{90}\text{Nb}$  gated on (a) 755-keV, (b) 813-keV, (c) 2063-keV, and (d) 1904-keV transitions. Some of the prominent  $\gamma$  rays are labeled with their energies in kilo-electron Volts. The  $\gamma$  rays marked with an asterisk are contaminations from  $^{91}\text{Nb}$  [16].

not seen in our experiment. About 20 new  $\gamma$  rays between high-spin states have been assigned to  $^{90}\text{Nb}$  and the level scheme has been extended up to an excitation energy of 8.095 MeV.

As shown in our level scheme, the  $9^-$ ,  $11^-$ , and  $12^-$  negative-parity states were well established in  $^{89}\text{Y}(\alpha, 3n)$  and  $^{90}\text{Zr}({}^3\text{He}, p2n)$  reactions [15]. The  $12^-$  state decays via a 607-keV  $M1$   $\gamma$  ray to the  $11^-$  state. The  $11^-$  state was reported as an isomer with a 440-ns lifetime [15] and is depopulated by the 1067-keV  $M2$  transition to the  $9^+$  state and by the 71-keV  $E2$  transition to the  $9^-$  state. The 71-keV  $\gamma$  ray has not been observed in the present experiment because of the high threshold set in the electronics. Other  $\gamma$  rays and their coincidence relationships have been observed in the present reaction.

All of the positive-parity states above the  $9^+$  state are new. Moreover, instead of the 1173-keV  $\gamma$  ray reported in Ref. [15], a 2063-keV  $10^+$ -to- $8^+$  transition was observed in the present work. Note that the 2063-keV  $\gamma$  ray should be also attributed to  $^{91}\text{Nb}$  [16]. The coincidence relationship of the 755-keV transition with the 813-, 1250-, and 2063-keV transitions, as

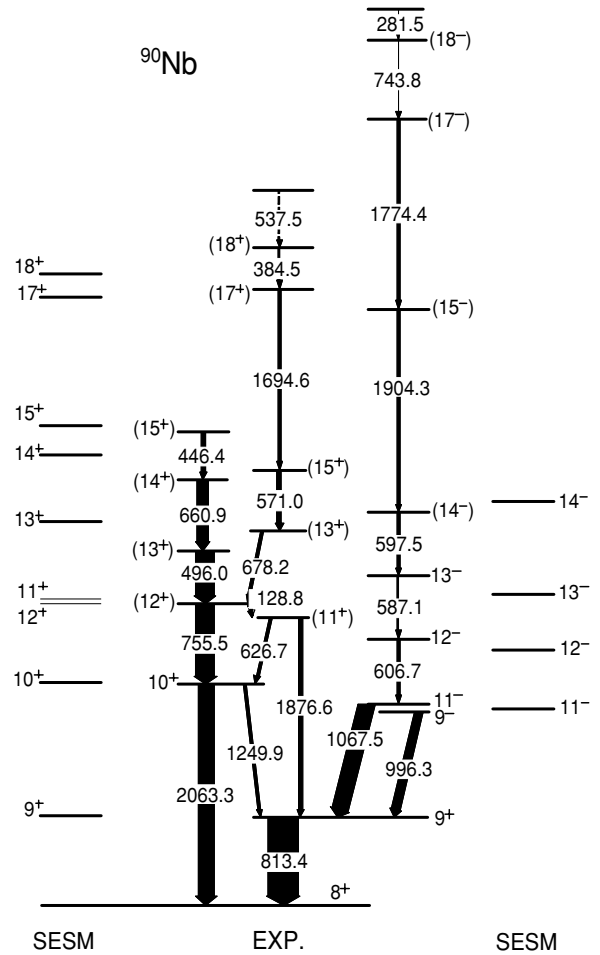


FIG. 2. Level scheme of  $^{90}\text{Nb}$  proposed from 80-MeV  $^{19}\text{F} + {}^{76}\text{Ge}$  reaction, compared with the results of semiempirical shell model (SESM) calculations, see text for details.

seen in Fig. 1, and the energy balance between these transitions also support our assignments.

**B.  $\gamma$ - $\gamma$  directional correlations**

Information on the multipole orders of  $\gamma$  rays can be deduced from the  $\gamma$ - $\gamma$  directional correlation of the oriented state (DCO method) [17]. To obtain the DCO ratios of the  $\gamma$  rays, the data were sorted off-line into an angle-related  $E_\gamma$ - $E_\gamma$  matrix by placing the events recorded in the detectors at  $90^\circ$  on the  $x$  axis, whereas the events recorded in the detectors at forward ( $48^\circ$ ) and backward ( $132^\circ$ ) angles were on the  $y$  axis. Here the DCO ratio  $R_{\text{DCO}}$  was defined as follows:

$$R_{\text{DCO}} = \frac{I(x, y)}{I(y, x)} = \frac{I_\gamma[\gamma(x), \gamma_g(y)]\varepsilon(\gamma_g)}{I_\gamma[\gamma(y), \gamma_g(x)]\varepsilon(\gamma)}$$

where  $I_\gamma[\gamma(x), \gamma_g(y)]$  is the intensity of  $\gamma$  rays on the  $x$  axis gated by  $\gamma_g$  on the  $y$  axis,  $I_\gamma[\gamma(y), \gamma_g(x)]$  is the intensity of  $\gamma$  rays on the  $y$  axis gated by  $\gamma_g$  on the  $x$  axis, and  $\varepsilon(\gamma_i)$  is the ratio of the efficiency of  $\gamma_i$  at  $90^\circ$  to that at forward ( $48^\circ$ ) and backward ( $132^\circ$ ) angles.

The 813.4- and 1067.5-keV  $\gamma$  rays were known to be dipole and quadrupole transitions, respectively, from previous experiments. Starting from these two transitions, the values of the

TABLE I.  $\gamma$  rays assigned to  $^{90}\text{Nb}$  in the present experiment, together with their relative intensities, DCO ratios, proposed multiplicities, the spins of the initial and final states, and the energies of the initial states.

$E_\gamma$ (keV) <sup>a</sup>	$I_\gamma$ <sup>b</sup>	$R_{\text{DCO}}$ <sup>c</sup>	$\sigma\lambda$ <sup>d</sup>	$J_i^\pi$	$J_f^\pi$	$E_i^e$ (keV)
813.4	100(10)	0.50(0.09)	$M1$	$9^+$	$8^+$	813.4
996.3	26.8(5.2)	0.88(0.67)	$E1$	$9^-$	$9^+$	1809.7
1067.5	52.1(7.2)	1.48(0.37)	$M2$	$11^-$	$9^+$	1880.9
1249.9	8.9(3.7)	0.78(0.37)	$M1$	$(10^+)$	$9^+$	2063.3
2063.3	56.3(7.5)	1.61(0.30)	$E2$	$(10^+)$	$8^-$	2063.3
606.7	8.1(2.8)	0.72(0.43)	$M1$	$12^-$	$11^-$	2487.8
1876.6	12.1(3.5)	1.97(1.60)	$E2$	$(11^+)$	$(9^+)$	2690.0
626.7	6.3(2.5)	1.30(0.64)	$E2$	$(11^+)$	$(10^+)$	2690.0
755.5	65.2(8.1)	1.35(0.51)	$E2$	$(12^+)$	$(10^+)$	2818.8
496.0	60.7(7.8)	0.57(0.21)	$M1$	$(13^+)_1$	$(12^+)$	3314.8
678.2	4.5(2.1)	0.22(0.36)	$M1$	$(13^+)_2$	$(12^+)$	3497.0
587.1	5.0(2.5)	0.35(0.29)	$M1$	$(13^-)$	$(12^-)$	3074.9
597.5	8.5(2.9)	0.66(0.35)	$M1$	$(14^-)$	$(13^-)$	3672.4
660.9	37.6(8.2)	0.43(0.20)	$M1$	$(14^+)$	$(13^+)_1$	3975.7
571.0	14.9(3.8)	0.78(0.52)	$(E2)^f$	$(15^+)_1$	$(13^+)_2$	4068.0
446.4	12.8(4.2)	0.56(0.53)	$M1$	$(15^+)_2$	$(14^+)$	4422.1
1694.6	7.0(2.6)	2.23(1.40)	$E2$	$(17^+)$	$(15^+)$	5762.6
384.5	5.3(2.3)	0.35(0.25)	$M1$	$(18^+)$	$(17^+)$	6147.1
1904.3	3.3(1.8)	0.49(0.31)	$M1$	$(15^-)$	$(14^-)$	5576.7
1774.4	6.6(2.6)	1.66(0.62)	$E2$	$(17^-)$	$(15^-)$	7351.1
743.8	2.1(1.4)	0.71(0.44)	$M1$	$(18^-)$	$(17^-)$	8094.9

<sup>a</sup>The error of the  $\gamma$ -ray energy is about 0.3 keV.

<sup>b</sup>Relative intensity derived from the total-projection spectrum and some of the gated spectra.

<sup>c</sup>DCO ratio  $R_{\text{DCO}}$  extracted from the spectrum gated on a quadrupole transition.

<sup>d</sup>Transition multipolarity deduced from the value of  $R_{\text{DCO}}$ .

<sup>e</sup>Energy of the initial state.

<sup>f</sup>The transition multipolarity was assigned by the systemic comparison with neighbor isotones and the shell-model calculation.

<sup>g</sup>The 128.8-, 281.5-, and 537.5-keV  $\gamma$  rays are too weak and are not listed in the table.

DCO ratios of some  $\gamma$  rays have been then extracted from the angle-related  $E_\gamma$ - $E_\gamma$  matrix after careful background subtractions. The DCO ratios of  $\gamma$  rays assigned to  $^{90}\text{Nb}$  in the present work are listed in Table I, where all the values were deduced from the spectra gated on nearby quadrupole transitions. The reliability of these analyses has been checked by the prompt  $\gamma$  rays of  $^{90,91}\text{Zr}$  whose multiplicities are already known. For the geometry of our detector array, if the gated  $\gamma$  ray is a quadrupole transition, a DCO ratio about 1.2 is expected for  $\Delta J = 2$  transitions and 0.5 for  $\Delta J = 1$  transitions.

### C. The assignment of spin and parity

The spins and parities of the levels in  $^{90}\text{Nb}$  are tentatively assigned according to the DCO ratios. Because electric dipole transitions are inhibited by a factor of  $10^4$  or more [18] in the mass  $\sim 90$  region, all the  $\gamma$  rays with DCO ratio about 0.5 listed in Table I have been tentatively assigned to be  $M1$  transitions, except for the 996-keV  $\gamma$  ray that has been already assigned to be an  $E1$  transition in  $^{89}\text{Y}(\alpha, 3n)$  and  $^{90}\text{Zr}(^3\text{He}, p2n)$  studies [15]. The reliability of such assignments has been checked by systematic comparisons with neighboring isotones and by the shell-model calculations discussed in next part.

The highest level reported in Ref. [15], whose spin-parity was not given, is now assigned as  $13^-$  according to the DCO ratio of 587-keV  $\gamma$  ray. Above the  $13^-$  state, five new cascade

transitions, i.e., 597, 1904, 1774, 743, and 281 keV, were observed for the first time. The coincidence spectrum gated on the 1904-keV  $\gamma$  ray is shown in Fig. 1(d). The spin values of the new levels were determined from the DCO ratios of the new transitions to be  $14^-$ ,  $15^-$ ,  $17^-$ , and  $18^-$ , whereas the spin of the highest level was not given because the intensity of 281-keV transition was too weak to be observed in our experiment.

The level sequence above the  $10^+$  state resembles a sequence in  $^{92}\text{Tc}$ . Based on this similarity and the DCO ratios of the 756, 497-, 660-, and 446-keV  $\gamma$  rays, and adopting the suggestion that  $E1$  transitions are highly inhibited in the mass  $\sim 90$  region [18], the levels at 2819, 3315, 3976, and 4422 keV are assigned as  $12^+$ ,  $13^+$ ,  $14^+$   $15^+$ , respectively. The level that deexcites by a 1877-keV  $\gamma$  ray to the  $9^+$  state and a 626-keV  $\gamma$  ray to the  $10^+$  state was assigned as  $11^+$  from the DCO ratios of the 626- and 1877-keV  $\gamma$  rays.

### III. DISCUSSION: SEMIEMPIRICAL SHELL-MODEL INTERPRETATION

The low-lying states of  $^{90}\text{Nb}$  have been well described by shell-model calculations [15] using the  $\pi(g_{9/2})^3\nu(g_{9/2})$  and  $\pi(p_{1/2})\pi(g_{9/2})^2\nu(g_{9/2})$  configurations. To understand the high-spin states of  $^{90}\text{Nb}$  observed in the present work, we have performed semiempirical shell-model (SESM) calculations

[19], which allow a truncation of shell-model configuration into simpler ones, where these simpler configurations correspond to specific levels in neighboring nuclei. In our calculation,  $^{90}\text{Zr}$  was chosen as the core, and the ground state of  $^{90}\text{Nb}$  was considered as one  $g_{9/2}$  proton particle and one  $g_{9/2}$  neutron hole outside the  $^{90}\text{Zr}$  core, i.e., the configuration  $\pi g_{9/2} \otimes \nu g_{9/2}^{-1}$ . The calculations were restricted in the model space  $\pi(1p_{1/2}, 0f_{5/2}, 0g_{9/2})\nu(0g_{9/2})$ , and only two-body interactions were taken into account. The single-particle energies and the residual interaction strength of particle-particle, particle-hole, hole-hole, and particle (hole)-core were extracted from the neighboring nuclei  $^{91}\text{Nb}$  [16],  $^{90}\text{Zr}$  [7],  $^{89}\text{Nb}$  [5],  $^{89}\text{Zr}$  [20],  $^{89}\text{Y}$  [21],  $^{88}\text{Y}$  [21], and  $^{87}\text{Sr}$  [22]. The calculated results are summarized in Table II.

As an example for negative-parity states, the  $12^-$  level is proposed as a four-quasiparticle state, dominated by the configuration  $\pi(p_{1/2}^{-1}g_{9/2}^2) \otimes \nu g_{9/2}^{-1}$ . Its energy can be decomposed as follows:

$$\begin{aligned}
E[^{90}\text{Nb}, 12^-, \pi g_{9/2} \otimes \nu(p_{1/2}^{-1}g_{9/2}^{-1}d_{5/2})] \\
= E(^{91}\text{Nb}, 17/2^-, \pi p_{1/2}^{-1}g_{9/2}^2) + E(^{89}\text{Zr}, 9/2^+, \nu g_{9/2}^{-1}) \\
+ \sum_{I_1=5,4} \left( \sqrt{(2 \times 17/2 + 1)(2I_1 + 1)} \begin{Bmatrix} 8 & 1/2 & 17/2 \\ 9/2 & 12 & I_1 \end{Bmatrix} \right)^2 \\
\times \Delta(I_1^-, \pi p_{1/2}^{-1} \nu g_{9/2}^{-1}) \\
+ \sum_{I_2=9,8} \left( \sqrt{(2 \times 17/2 + 1)(2I_2 + 1)} \begin{Bmatrix} 4 & 9/2 & 17/2 \\ 9/2 & 12 & I_2 \end{Bmatrix} \right)^2 \\
\times \Delta(I_2^+, \pi g_{9/2} \nu g_{9/2}^{-1}) \\
+ \sum_{I_3=8,7} \left( \sqrt{(2 \times 17/2 + 1)(2I_3 + 1)} \begin{Bmatrix} 5 & 9/2 & 17/2 \\ 9/2 & 12 & I_3 \end{Bmatrix} \right)^2 \\
\times \Delta(I_3^+, \pi g_{9/2} \nu g_{9/2}^{-1}) - S1 = 2.382 \text{ MeV},
\end{aligned}$$

where  $E$  is the corresponding level energy and  $\Delta$  is the two-body interaction between the two valence nucleons and can be extracted from the neighboring nuclei as follows:

$$\begin{aligned}
\Delta(4^-, \pi p_{1/2}^{-1} \nu g_{9/2}^{-1}) &= E(^{88}\text{Y}, 4^-, \pi p_{1/2}^{-1} \nu g_{9/2}^{-1}) \\
&\quad - E(^{89}\text{Zr}, 9/2^+, \pi g_{9/2}) \\
&\quad - E(^{89}\text{Y}, 1/2^-, \nu p_{1/2}^{-1}) - S2, \\
\Delta(5^-, \pi p_{1/2}^{-1} \nu g_{9/2}^{-1}) &= E(^{88}\text{Y}, 5^-, \pi p_{1/2}^{-1} \nu g_{9/2}^{-1}) \\
&\quad - E(^{89}\text{Zr}, 9/2^+, \pi g_{9/2}) \\
&\quad - E(^{89}\text{Y}, 1/2^-, \nu p_{1/2}^{-1}) - S2, \\
\Delta(9^+, \pi g_{9/2} \nu g_{9/2}^{-1}) &= E(^{90}\text{Nb}, 9^+, \pi g_{9/2} \nu g_{9/2}^{-1}) \\
&\quad - E(^{91}\text{Nb}, 9/2^+, \pi g_{9/2}) \\
&\quad - E(^{89}\text{Zr}, 9/2^+, \nu g_{9/2}^{-1}) - S3, \\
\Delta(8^+, \pi g_{9/2} \nu g_{9/2}^{-1}) &= E(^{90}\text{Nb}, 8^+, \pi g_{9/2} \nu g_{9/2}^{-1}) \\
&\quad - E(^{91}\text{Nb}, 9/2^+, \pi g_{9/2}) \\
&\quad - E(^{89}\text{Zr}, 9/2^+, \nu g_{9/2}^{-1}) - S3,
\end{aligned}$$

TABLE II. Dominant configurations proposed from the semiempirical shell-model calculations for the high-spin states in  $^{90}\text{Nb}$  observed in the present work, together with the calculated level energies.

$J^\pi$	$E_{\text{exp}}$ (keV)	Configuration	$E_{\text{calc}}$ (keV)
Negative-parity states			
$11^-$	1881	$\pi(p_{1/2}^{-1}g_{9/2}^2) \otimes \nu(g_{9/2})^{-1}$	1834
$12^-$	2488	$\pi(p_{1/2}^{-1}g_{9/2}^2) \otimes \nu(g_{9/2})^{-1}$	2382
$13^-$	3075	$\pi(p_{1/2}^{-1}g_{9/2}^2) \otimes \nu(g_{9/2})^{-1}$	2902
$14^-$	3672	$\pi(f_{5/2}^{-1}g_{9/2}^2) \otimes \nu(g_{9/2})^{-1}$	3770
$15^-$	5577	$\pi g_{9/2} \otimes \nu(f_{5/2}^{-1}g_{9/2}^{-1}g_{7/2})$	— <sup>a</sup>
Positive-parity states			
$9^+$	813	$\pi g_{9/2} \otimes \nu g_{9/2}^{-1}$	834
$10^+$	2063	$(\pi g_{9/2} \otimes \nu g_{9/2}^{-1}; 8^+) \otimes 2^+$	2083
$11^+$	2690	$(\pi g_{9/2} \otimes \nu g_{9/2}^{-1}; 9^+) \otimes 2^+$	2857
$12^+$	2819	$\pi g_{9/2}^3 \otimes \nu g_{9/2}^{-1}$	2850
$13^+$	3315	$\pi g_{9/2}^3 \otimes \nu g_{9/2}^{-1}$	3580
$14^+$	3976	$\pi g_{9/2}^3 \otimes \nu g_{9/2}^{-1}$	4216
$15^+$	4422	$\pi g_{9/2}^3 \otimes \nu g_{9/2}^{-1}$	4489
$17^+$	5761	$\pi g_{9/2}^5 \otimes \nu g_{9/2}^{-1}$	5687
$18^+$	6145	$\pi(f_{5/2}^{-1}p_{1/2}^{-1}g_{9/2}^3) \otimes \nu g_{9/2}^{-1}$	5900

<sup>a</sup>The energy of the state has not been extracted the absence of the  $17/2^-$  state in neighbor nuclei  $^{89}\text{Zr}$  [21], see text for details.

$$\begin{aligned}
\Delta(7^+, \pi g_{9/2} \nu g_{9/2}^{-1}) &= E(^{90}\text{Nb}, 7^+, \pi g_{9/2} \nu g_{9/2}^{-1}) \\
&\quad - E(^{91}\text{Nb}, 9/2^+, \pi g_{9/2}) \\
&\quad - E(^{89}\text{Zr}, 9/2^+, \nu g_{9/2}^{-1}) - S3.
\end{aligned}$$

The mass windows are as follows:

$$\begin{aligned}
S1 &= B(^{91}\text{Nb}) + B(^{89}\text{Zr}) - B(^{90}\text{Zr}) - B(^{90}\text{Nb}), \\
S2 &= B(^{88}\text{Y}) + B(^{90}\text{Zr}) - B(^{89}\text{Y}) - B(^{89}\text{Zr}), \\
S3 &= B(^{90}\text{Zr}) + B(^{90}\text{Nb}) - B(^{91}\text{Nb}) - B(^{89}\text{Zr}),
\end{aligned}$$

and  $B(X)$  is the binding energy of the nucleus  $X$ . The calculated energy of 2.382 MeV for the  $12^-$  state is quite close to that of the experimental value (2.488 MeV). Using the same method, the configuration  $\pi(p_{1/2}^{-1}g_{9/2}^2) \otimes \nu g_{9/2}^{-1}$  is proposed for the  $11^-$  and  $13^-$  states and  $\pi(f_{5/2}^{-1}g_{9/2}^2) \otimes \nu(g_{9/2})^{-1}$  is suggested for the  $14^-$  state. The calculated results listed in Table II agree well with the experimental observations. For the  $15^-$  state, a possible configuration is  $\pi g_{9/2} \otimes \nu(f_{5/2}^{-1}g_{9/2}^{-1}g_{7/2})$ . Because of the absence of the  $17/2^-$  state in  $^{89}\text{Zr}$ , we could not extract the two-body interaction between the neutrons to get a value for this state. From the calculations for the negative-parity states, it is noted that the angular momentum of the  $13^-$  and  $14^-$  states arises mainly from the excitation of one proton to the  $g_{9/2}$  orbital either from the  $p_{1/2}$  orbital or from the  $f_{5/2}$  orbital inside the inner core, whereas the valence neutron hole resides in the  $g_{9/2}$  orbital.

For the positive-parity states, the  $10^+$  and  $11^+$  levels are proposed to result from the coupling of  $\pi g_{9/2} \otimes \nu g_{9/2}^{-1}$  with the  $2^+$  quadrupole phonon state of  $^{90}\text{Zr}$  [7]. Under this assumption, the energy of the  $10^+$  state can be decomposed as follows:

$$\begin{aligned} E(^{90}\text{Nb}, 10^+, [\pi g_{9/2} \otimes \nu g_{9/2}^{-1}]_8^+ \otimes [^{90}\text{Zr}]_{2^+}) \\ = E(^{91}\text{Nb}, 13/2^+, \pi g_{9/2} \otimes 2^+) + E(^{89}\text{Zr}, 13/2^+, \nu g_{9/2}^{-1} \otimes 2^+) \\ - E(^{90}\text{Zr}, 2^+) + \Delta(8^+, \pi g_{9/2} \otimes \nu g_{9/2}^{-1}) - S1 = 2.083 \text{ MeV}, \end{aligned}$$

where the two-body interaction  $\Delta(8^+, \pi g_{9/2} \otimes \nu g_{9/2}^{-1})$  is the same as defined previously.

The value of 2.083 MeV for the  $10^+$  state is very close to the present experimental value of 2.063 MeV, as shown in Fig. 2. This result again confirms the experimental assignment of  $10^+$  level, followed by a 2063-keV  $\gamma$ -ray transition to the  $8^+$  state. In fact, the shell-model calculations in Refs. [6] and [18] predicted yrast  $10^+$  states lying at 2.123 and 2.025 MeV, respectively. Our results support the assignment of the  $10^+$  state given by previous shell-model calculations and a more reliable level energy is given by our calculation. The energy of the  $11^+$  state was calculated using the same method and is listed in Table II.

For the states above the  $11^+$  state, the excitation of proton particles from the inner core is suggested in the calculations. The states of  $12^+$ ,  $13^+$ ,  $14^+$ , and  $15^+$  were proposed to be four-quasiparticle configurations  $\pi g_{9/2}^3 \otimes \nu g_{9/2}^{-1}$ , corresponding to the excitation of a pair of protons from the inner core to the  $g_{9/2}$  orbital. The calculated results of these states are listed in Table II.

The configuration of the  $17^+$  state was supposed to be a six-quasiparticle configuration,  $\pi g_{9/2}^5 \otimes \nu g_{9/2}^{-1}$ , the same as its isotone  $^{92}\text{Tc}$ , and its level energy can be calculated as follows:

$$\begin{aligned} E(^{90}\text{Nb}, 17^+, \pi g_{9/2}^5 \otimes \nu g_{9/2}^{-1}) \\ = E[^{91}\text{Nb}, 25/2^+, \pi(g_{9/2}^5)] + E(^{89}\text{Zr}, \nu g_{9/2}^{-1}) - S1 \\ + \Delta(9^+, \pi g_{9/2} \nu g_{9/2}^{-1}) + \Delta(8^+, \pi g_{9/2} \nu g_{9/2}^{-1}) \\ + \Delta(7^+, \pi g_{9/2} \nu g_{9/2}^{-1}). \end{aligned}$$

The three terms of interaction can be extracted as a whole from the following equation:

$$\begin{aligned} E(^{92}\text{Tc}, 17^+, \pi g_{9/2}^3 \otimes \nu g_{9/2}^{-1}) \\ = E[^{93}\text{Tc}, 25/2^+, \pi(g_{9/2}^3)] + E(^{91}\text{Mo}, \nu g_{9/2}^{-1}) - S4 \\ + \Delta(9^+, \pi g_{9/2} \nu g_{9/2}^{-1}) + \Delta(8^+, \pi g_{9/2} \nu g_{9/2}^{-1}) \\ + \Delta(7^+, \pi g_{9/2} \nu g_{9/2}^{-1}), \end{aligned}$$

where  $S4 = B(^{93}\text{Tc}) + B(^{91}\text{Mo}) - B(^{92}\text{Mo}) - B(^{92}\text{Tc})$ .

The  $18^+$  state was suggested as a six-quasiparticle configuration,  $\pi(f_{5/2}^{-1} p_{1/2}^{-1} g_{9/2}^3) \otimes \nu g_{9/2}^{-1}$ , which is analogous to the  $27/2^+$  level of  $^{91}\text{Nb}$ . The energy of this level was decomposed

as follows:

$$\begin{aligned} E[^{90}\text{Nb}, 18^+, \pi(f_{5/2}^{-1} p_{1/2}^{-1} g_{9/2}^3) \otimes \nu g_{9/2}^{-1}] \\ = E[^{91}\text{Nb}, 27/2^+, \pi(f_{5/2}^{-1} p_{1/2}^{-1} g_{9/2}^3)] + E(^{89}\text{Zr}, \nu g_{9/2}^{-1}) \\ - S1 + \Delta(7^-, \pi f_{5/2}^{-1} \nu g_{9/2}^{-1}) + \Delta(5^-, \pi p_{1/2}^{-1} \nu g_{9/2}^{-1}) \\ + \Delta(9^+, \pi g_{9/2} \nu g_{9/2}^{-1}) + \Delta(8^+, \pi g_{9/2} \nu g_{9/2}^{-1}) \\ + \Delta(7^+, \pi g_{9/2} \nu g_{9/2}^{-1}) = 5.900 \text{ MeV}. \end{aligned}$$

Here the two-body interactions  $\Delta(9^+, \pi g_{9/2} \nu g_{9/2}^{-1})$ ,  $\Delta(8^+, \pi g_{9/2} \nu g_{9/2}^{-1})$  and  $\Delta(7^+, \pi g_{9/2} \nu g_{9/2}^{-1})$  are the same as defined before and

$$\begin{aligned} \Delta(7^-, \pi f_{5/2}^{-1} \nu g_{9/2}^{-1}) &= E(^{88}\text{Y}, 7^-, \pi f_{5/2}^{-1} \nu g_{9/2}^{-1}) \\ &\quad - E(^{89}\text{Zr}, 9/2^+, \nu g_{9/2}^{-1}) \\ &\quad - E(^{89}\text{Y}, 5/2^-, \pi f_{5/2}^{-1}) - S5, \\ \Delta(5^-, \pi p_{1/2}^{-1} \nu g_{9/2}^{-1}) &= E(^{88}\text{Y}, 5^-, \pi p_{1/2}^{-1} \nu g_{9/2}^{-1}) \\ &\quad - E(^{89}\text{Zr}, 9/2^+, \nu g_{9/2}^{-1}) \\ &\quad - E(^{89}\text{Y}, 1/2^-, \pi p_{1/2}^{-1}) - S5. \end{aligned}$$

with the mass window

$$S5 = B(^{89}\text{Zr}) + B(^{89}\text{Y}) - B(^{90}\text{Zr}) - B(^{88}\text{Y}).$$

For other even higher spin states, i.e., the levels above the  $18^+$  state, six- or even more quasiparticle configurations, including excitations across the  $N = 50$  and/or  $Z = 50$  shell gaps should be involved. The decomposition calculations of these levels were not successful because of the shortage of the level information of neighboring nuclei.

#### IV. SUMMARY

The high-spin states of  $^{90}\text{Nb}$  have been studied via the reaction  $^{76}\text{Ge}(^{19}\text{F}, 5n)^{90}\text{Nb}$  at a beam energy of 80 MeV. Based on the measurements of  $\gamma$ -ray intensities, DCO ratios, and  $\gamma$ - $\gamma$  coincidences, 20 new  $\gamma$  transitions have been assigned to  $^{90}\text{Nb}$  and its level scheme has been extended to high-spin states at an excitation energy of 8.095 MeV and spin of  $18\hbar$ . The experimental results have been well reproduced with semiempirical shell-model calculations using a configuration space,  $\pi(1p_{1/2}, 0f_{5/2}, 0g_{9/2})\nu(0g_{9/2})$ , showing that the excitation of protons plays an important role in the generation of the high angular momentum in  $^{90}\text{Nb}$ . However, to improve the calculated results for the higher spin levels, a larger configuration space and greater particle excitation across the  $N = 50$  and/or  $Z = 50$  shell gaps must be included in the calculations.

#### ACKNOWLEDGMENTS

The authors wish to acknowledge the staff of the HI-13 tandem accelerator in the China Institute of Atomic Energy

for providing good beam conditions. The authors are greatly indebted to Dr. G. J. Xu for preparing the targets. This work was supported by the National Natural Science Foundation of

China under grant nos. 10175090, 10105015, and 10375092, and by the Major State Basic Research Development Program under contract no. TG2000077405.

- 
- [1] K. Muto, T. Shimano, and H. Horie, *Phys. Lett.* **B135**, 349 (1984).
- [2] E. A. Stefanova, M. Danchev, and R. Schwenger *et al.*, *Phys. Rev. C* **65**, 034323 (2002).
- [3] E. A. Stefanova, R. Schwenger, J. Reif *et al.*, *Phys. Rev. C* **62**, 054314 (2000).
- [4] Xiangdong Ji and B. H. Wildental, *Phys. Rev. C* **37**, 1256 (1988).
- [5] Pragya Singh, R. G. Pillay, J. A. Sheikh, and H. E. Devare, *Phys. Rev. C* **48**, 1609 (1993).
- [6] R. Gross and Afrenkel, *Nucl. Phys.* **A267**, 85 (1976).
- [7] E. K. Warburton, J. W. Olness, C. J. Lister *et al.*, *Phys. Rev. C* **31**, 1184 (1985).
- [8] Pragya Singh, R. G. Pillay, J. A. Sheikh *et al.*, *Phys. Rev. C* **45**, 2161 (1992).
- [9] N. S. Pattabiraman, S. N. Chintalapudi, S. S. Ghugre *et al.*, *Phys. Rev. C* **65**, 044324 (2002).
- [10] R. Schubart, A. Jungclaus, A. Harder *et al.*, *Nucl. Phys.* **A591**, 515 (1995).
- [11] S. S. Ghugre, S. B. Patel, and R. K. Bhowmik, *Phys. Rev. C* **51**, 1136 (1995).
- [12] H. A. Roth, S. E. Arnell, D. Foltescu *et al.*, *Phys. Rev. C* **50**, 1330 (1994).
- [13] F. Puhlhofer, *Nucl. Phys.* **A280**, 267 (1977).
- [14] D. C. Radford, *Nucl. Instrum. Methods Phys. Res. A* **361**, 297 (1995).
- [15] C. A. Fields, F. W. N. De Boer, J. J. Kraushaar *et al.*, *Nucl. Phys.* **A363**, 311 (1981).
- [16] C. A. Fields, J. J. Kraushaar, R. A. Ristinen *et al.*, *Nucl. Phys.* **A326**, 55 (1979).
- [17] Li Guang-sheng, *Chin. Phys. Lett.* **16**, 796 (1999).
- [18] F. J. D. Serduke, R. D. Lawson, and D. H. Gloeckner, *Nucl. Phys.* **A256**, 45 (1976).
- [19] J. Blomqvist and L. Rydström, *Physica Scripta* **31**, 31 (1985).
- [20] J. Biping, J. Ernst, F. Rauch *et al.*, *Nucl. Phys.* **A230**, 221 (1974).
- [21] E. K. Warburton, J. W. Olness, C. J. Lister *et al.*, *J. Phys. G* **12**, 1017 (1986).
- [22] L. P. Ekstrom, G. D. Jones, F. Keans *et al.*, *J. Phys. G* **7**, 85 (1981).